Title

The X-ray crystal structure of human endothelin 1, a polypeptide hormone regulator of blood pressure.

Journal

Acta Crystallographica Section F: Structural Biology Communications, 75(Pt 1)

Authors

Mcpherson, Alexander

Larson, Steven

Publication Date

2019

DOI

10.1107/S2053230X18016011

Peer reviewed

STRUCTURAL BIOLOGY COMMUNICATIONS

ISSN 2053-230X

The X-ray crystal structure of human endothelin 1, a polypeptide hormone regulator of blood pressure

Alexander McPherson* and Steven B. Larson

Molecular Biology and Biochemistry, University of California Irvine, McGaugh Hall, Irvine, CA 92697-3900, USA. *Correspondence e-mail: amcphers@uci.edu

Received 6 August 2018
Accepted 12 November 2018

Edited by R. L. Stanfield, The Scripps Research Institute, USA

Keywords: endothelin; blood pressure; vasoconstrictors; polypeptide hormones; twinned crystals; crystallographic archeology.

PDB reference: endothelin, 6dk5

Supporting information: this article has supporting information at journals.iucr.org/f

Human endothelin is a 21-amino-acid polypeptide, constrained by two intra-chain disulfide bridges, that is made by endothelial cells. It is the most potent vasoconstrictor in the body and is crucially important in the regulation of blood pressure. It plays a major role in a host of medical conditions, including hypertension, diabetes, stroke and cancer. Endothelin was crystallized 28 years ago in the putative space group $P6_122$, but the structure was never successfully solved by X-ray diffraction. Using X-ray diffraction data from 1992, the structure has now been solved. Assuming a unit cell belonging to space group $P6_1$ and a twin fraction of 0.28, a solution emerged with two, almost identical, closely associated molecules in the asymmetric unit. Although the data extended to beyond 1.8 Å resolution, a model containing 25 waters was refined to 1.85 Å resolution with an R of 0.216 and an R_{free} of 0.284. The disulfide-constrained 'core' of the molecule, amino-acid residues 1–15, has a main-chain conformation that is essentially the same as endothelin when bound to its receptor, but many side-chain rotamers are different. The carboxy-terminal 'tail' comprising amino-acid residues 16–21 is extended as when receptor-bound, but it exhibits a different conformation with respect to the 'core'. The dimer that comprises the asymmetric unit is maintained almost exclusively by hydrophobic interactions and may be stable in an aqueous medium.

1. Introduction

Endothelin is a 21-amino-acid polypeptide hormone of molecular mass 2492 Da that is secreted by mammalian endothelial cells both in culture and in living tissues (Hickey *et al.*, 1985; Yanagisawa & Masaki, 1989; Yanagisawa, Kurihara *et al.*, 1988). The polypeptide, the amino-acid sequence of which is shown in Fig. 1, contains four cysteine residues that spontaneously form two intra-chain disulfide bonds. Thus, the molecule is composed of a highly constrained 'head group' or 'core' of 15 amino-acid residues and a flexible carboxy-terminal 'tail' of six, mostly hydrophobic, amino-acid residues. The carboxy-terminal tryptophan has been shown to be essential for hormone activity (Shihoya *et al.*, 2016).

There are currently three known variants of endothelin, designated endothelin 1 (ET-1), endothelin 2 (ET-2) and endothelin 3 (ET-3), with ET-1 being the predominant isoform. ET-2 differs in sequence from ET-1 at only two positions, where Leu6→Trp6 and Met7→Leu7. ET-3 differs more, with the replacements Ser2→Thr2, Ser4→Phe4, Ser5→Thr5, Ser6→Tyr6, Met7→Lys7, Val16→Leu16 and Phe18→Tyr18. The same disulfides, Cys1–Cys15 and Cys3–Cys11, are formed in all endothelins, even when the polypeptides are produced by recombinant or synthetic means (Yanagisawa, Inoue *et al.*, 1988). Endothelin is very similar in

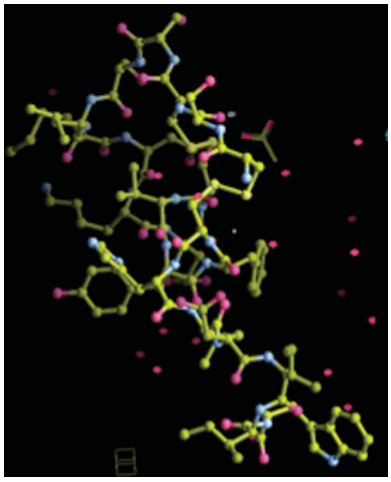

Cys-Ser-**Cys**-Ser-Ser-Leu-Met-Asp-Lys-Gly-**Cys**-Val-Tyr-Phe-**Cys**-*His-Leu-Asp-Ile-Ile-Trp*

1 5 10 15 20

Figure 1
The amino-acid sequence of endothelin 1 is shown. The cysteine residues that form the disulfide bridges (Cys1–Cys15 and Cys3–Cys11) are shown in bold. The underlined portion of the sequence represents the 'core' of the molecule

activity to a class of animal toxins known as sarafotoxins that are principally found in snakes and are also very powerful vasoconstrictors (Kloog *et al.*, 1988; Sokolovsky, 1995).

In humans, endothelins are initially produced as longer polypeptides of 39 amino-acid residues that are subsequently cleaved proteolytically to generate the physiologically active species. Endothelins bind in a virtually irreversible manner (Shihoya *et al.*, 2016) to a set of structurally similar, smooth muscle receptors that are GPCRs (Sokolovsky, 1995; Yanagisawa & Masaki, 1989; Yanagisawa, Inoue *et al.*, 1988). The currently known receptors are designated ET_A, ET_{B1}, ET_{B2} and ET_C. Each combination of an endothelin type with a receptor type produces a unique or modulated physiological effect (Maguire *et al.*, 2012; Maguire, 2016).

Endothelin is of profound physiological and medical importance as it is the most potent vasoconstrictor in the human body and is a crucial regulator of blood pressure, in addition to many associated functions that are too numerous to review here (Davenport *et al.*, 2016; Ducancel, 2005). It has been definitively implicated in a host of diseases that include hypertension (Dhaun *et al.*, 2008; Rautureau & Schiffrin, 2012; Touyz & Schiffrin, 2003), stroke (Kuhn *et al.*, 2006 March), a range of cardiovascular diseases (Gray & Webb, 1996), diabetes (Potenza *et al.*, 2009; Shemyakin *et al.*, 2010) and cancer (Bagnato & Rosanò, 2008). The molecule has been the object of intense pharmacological efforts to produce clinically effective and safe agonists and antagonists (Cody & Doherty, 1995; Lüscher & Barton, 2000; Maguire, 2016), including structure-based drug design (Klabunde & Hessler, 2002). Unfortunately, these efforts have shown only modest success. Currently, endothelin-based drugs are only in wide clinical use for pulmonary arterial hypertension and scleroderma-related digital ulcers (Kohan *et al.*, 2012).

An X-ray crystal structure of free human endothelin crystallized from water was reported in 1994 (PDB entry 1edn; Janes *et al.*, 1994). More recently, the entire crystal structure of ET-1 complexed with the receptor ET_B was described at a resolution of 2.3 Å (PDB entry 5glh), along with the corresponding structure of the uncomplexed receptor (PDB entry 5gli), thereby allowing the delineation of the conformational changes of the receptor that occur upon hormone binding (Shihoya *et al.*, 2016). When the endothelin structure extracted from PDB entry 5glh is superimposed on that from PDB entry 1edn, substantial differences in conformation are apparent in the 'core' 15 amino-acid residues and especially in the flexible carboxy-terminal tail. The tail in PDB entry 5ghl is fully extended, while that in PDB entry 1edn assumes a helical conformation. There are also significant conflicts between the model in PDB entry 1edn and the results of several studies of the structure of endothelin using NMR (Anderson *et al.*, 1992; Hewage *et al.*, 1997; Saudek *et al.*, 1989). These were ascribed mainly to conformational flexibility in the 'tail' region (Wallace *et al.*, 1995).

More than 28 years ago, we crystallized human endothelin at 37°C using 2-methyl-2,4-pentanediol (MPD) as a precipitant (Waller *et al.*, 1992). An extensive series of X-ray data sets were recorded at that time from native crystals and from a number of heavy-atom-derivative trials. The crystals, which were in the putative space group $P6_122$, resisted our best efforts to solve their structure using both molecular replacement and isomorphous replacement, and we never solved the crystal structure. The data were subsequently archived and the project was eventually shelved.

Given the advances in mathematical approaches, computers and software tools for crystallography developed in the past 28 years, and the appearance of a new probe model (from PDB entry 5glh), we retrieved the original X-ray diffraction data from our archives and resurrected the analysis. This time we were successful in solving the structure. We might thus consider this investigation a piece of 'crystallographic archeology'. There were two crucial reasons why we failed 28 years ago but now succeeded. Most importantly, we eventually deduced that the crystals did not belong to space group $P6_122$ as originally believed, but to $P6_1$, and the crystals exhibited a twin fraction of about 0.28 according to the *L*-test (Padilla & Yeates, 2003). The second factor was that we now had an endothelin model extracted from the receptor complex structure (PDB entry 5glh) for use as a probe in molecular-replacement searches. As described below, the combination of these two factors led almost immediately to an endothelin crystal structure.

2. Materials and methods

Details of the crystallization have been given previously (Waller *et al.*, 1992), but some description is appropriate here. The lyophilized polypeptide was dissolved in water at 37°C and crystals were grown over a period of 3–10 days by sitting-drop vapor diffusion using Cryschem plates (Hampton Research, Aliso Viejo, California, USA). The reservoirs consisted of 20–25% 2-methyl-2,4-pentanediol (MPD) buffered at pH 6.5 with 0.1 *M* MES adjusted with weak acetic acid. The drops were composed of 4 µl of the stock polypeptide solution plus 2 µl 0.2 *M* MES pH 6.5 and 6 µl reservoir solution. The plates were placed at 37°C until hexagonal prismatic crystals grew. These were about 400 µm in length and 150 µm wide in the best cases. The crystals had unit-cell parameters $a = b = 27.4$, $c = 79.6$ Å. Assuming that the unit cell contained 12 endothelin molecules, the V_M of 1.71 Å^3 Da^{-1} implies a solvent content of about 29%, with two molecules in the asymmetric unit of the $P6_1$ unit cell.

Table 1
Data collection, processing and scaling.

Values in parentheses are for the outer shell.

X-ray source	Rigaku RU-200 rotating anode
Detector	SDMS dual multiwire detectors
Molecules in asymmetric unit	2
Mosaicity (°)	0.8
Resolution (Å)	80.0–1.85 (1.89–1.85)
No. of observations	17597
No. of unique reflections	2291 (313)
X-ray wavelength (Å)	1.54
$CC_{1/2}$	0.947 (0.529)
R_{merge}	0.257 (0.540)
R_{meas}	0.283 (0.643)
$R_{p.i.m.}$	0.086 (0.295)
Completeness (%)	99.6 (62.4)
Multiplicity	7.7 (4.2)
$\langle I/\sigma(I)\rangle$	6.3 (2.2)
No. of batches	11
No. of crystals	2

Table 2
Refinement and model.

No. of reflections, work set	2881
No. of reflections, test set	143 (5.9%)
R_{work}	0.216
R_{free}	0.284
Mean B factor, overall (Å^2)	32.6
R.m.s.d., bonds (Å)	0.005
R.m.s.d., angles (°)	1.32
R.m.s.d., chiral volumes (Å^3)	0.061
Ramachandran outliers	2 (per asymmetric unit)
Rotamer outliers	0
Twinning fraction	0.28
TLS applied	No
B factors	Isotropic
No. of waters in asymmetric unit	25

Crystals were mounted by conventional means in 0.5 mm quartz capillaries (McPherson, 1982) and X-ray diffraction data were recorded at room temperature using a Rigaku RU-200 generator operated at 40 kV and 30 mA fitted with a Supper graphite crystal monochromator. The detectors were twin San Diego Multiwire Systems (SDMS) detectors at a crystal-to-detector distance of 420 mm. The images were processed with software provided by SDMS (Howard *et al.*, 1985). Structure-factor amplitudes were obtained by scaling and merging intensities from the archived `.ARC` files using *AIMLESS* (Evans, 2006, 2011; Blessing, 1995) to yield comprehensive data sets (Table 1). The X-ray data extended beyond 1.8 Å resolution, but only data to 1.85 Å resolution were included in the final refinement.

Although most current peptide structures are reported at near-atomic resolution, this was not possible in the current investigation, although the estimated coordinate errors are nevertheless a small fraction of an ångström. Endothelin, at 21 amino-acid residues, is neither a peptide nor a protein but falls in the intermediate range. As a consequence, the data from the crystals decline in average intensity at about 1.8 Å resolution and have a mosaicity of about 0.8°, which is common for hydrated proteins. On the other hand, because of the small-molecule properties and unusually low solvent volume, the molecules experience many more close intermolecular contacts than are found in most protein structures.

The structure of the enzyme in the hexagonal crystals was solved by molecular replacement using *Phaser* (McCoy *et al.*, 2007) once it was realized that the space group was $P6_1$ and that the crystals were twinned (with a twin fraction of 0.28 according to the *L*-test; Padilla & Yeates, 2003). The model of endothelin extracted from the ET_B–endothelin complex (PDB entry 5glh) was used as a probe. Rebuilding and most graphical operations relied on *Coot* (Emsley *et al.*, 2010), as did the quantitative comparison of models. Refinement of the model of the polypeptide (see Table 2) was carried out using *REFMAC*5 (Murshudov *et al.*, 2011) from the *CCP*4 suite (Winn *et al.*, 2011) based on a maximum-likelihood approach (Murshudov *et al.*, 2011; Read, 2001). The illustrations were prepared using *Coot*.

The number of observations (F_{hkl}) for a crystal is an inverse function of the unit-cell volume and, given the low solvent content and the small volume of the endothelin unit cell, the number of observations, although reasonable, may otherwise appear low. The number of observations per parameter (x, y, z, B) is about 2, but the maintenance of NCS twofold restraints means that effectively it is closer to 4. In addition, the many chemical and physical restraints imposed on the model, which are classically treated as observations, make it difficult to know precisely the ratio of observations to parameters, but it must be well beyond 4. In any case, the ratio for this investigation is within the range for most protein structure refinements.

3. Results and discussion

Approximately 15 X-ray data sets were recorded between 1992 and 1994 and were collected using twin SDMS multiwire detectors with a Rigaku rotating-anode source (see Table 1). These were state-of-the-art instruments at the time and were entirely adequate for protein crystal structure analysis, although hardly comparable to today's sources and detectors. Data sets for minimal, similar twin fractions were scaled together (Evans, 2006; Evans & Murshudov, 2013) to give a single comprehensive data set that extended to 1.8 Å resolution (see Table 1), although we chose to cut off the data used in refinement at 1.85 Å. Initially, the data were again treated as arising from a unit cell of space group $P6_122$ (according to the assessment of *AIMLESS*, although this was accompanied by a warning of likely twinning) with a single endothelin molecule in the asymmetric unit. After weeks of fruitless searching with molecular replacement using *Phaser* (Read, 2001; Storoni *et al.*, 2004; McCoy *et al.*, 2005, 2007) for a model that was refineable with *REFMAC*5 (Murshudov *et al.*, 1996, 1997, 2011), this assumption was abandoned. The data were rescaled and re-indexed in space group $P6_1$ with two molecules in the asymmetric unit.

The molecular-replacement program *Phaser* (McCoy *et al.*, 2007) from the *CCP*4 suite (Winn *et al.*, 2011) almost immediately produced a unique two-molecule solution for the asymmetric unit using the structure of endothelin from PDB entry 5glh as a search model. This solution refined without incident in space group $P6_1$ using amplitude detwinning in

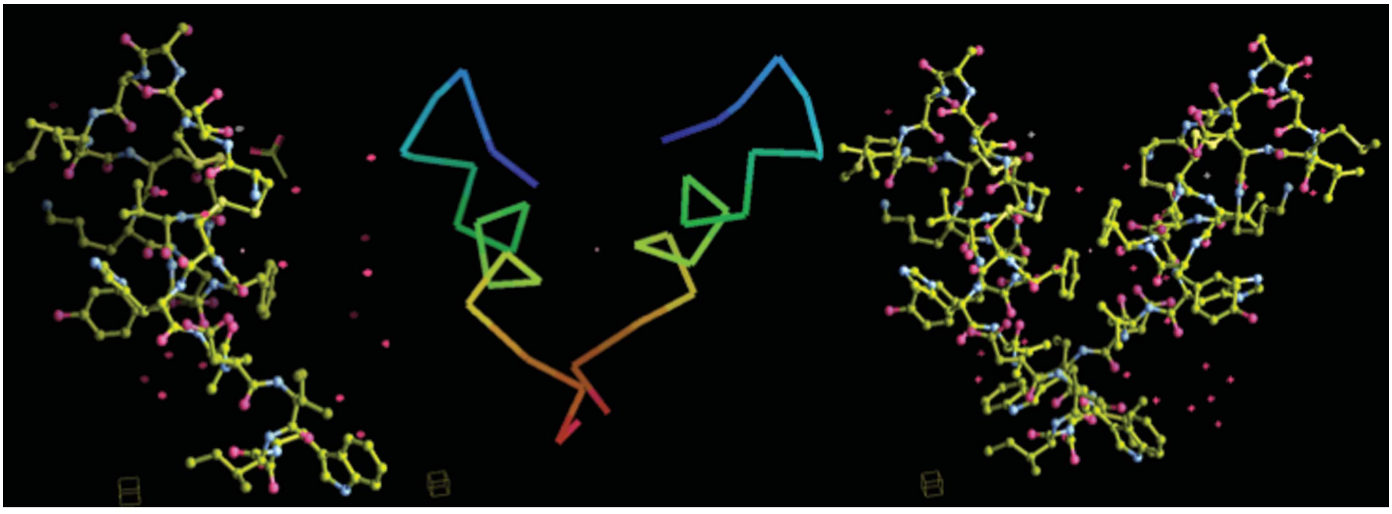

(*a*) (*b*) (*c*)

Figure 2
The model. (*a*) A single monomer of endothelin 1 with all atoms and associated water molecules. (*b*) A rainbow representation of the two endothelin molecules comprising the asymmetric unit of the crystal and representing a putative dimer. The amino-terminus is in blue and the carboxy-terminus is in red. (*c*) An all-atom plus waters representation of the pair of endothelin molecules comprising the crystallographic asymmetric unit. The molecules are all in the same orientation. C atoms are yellow, O atoms red and N atoms blue.

*REFMAC*5 (Murshudov *et al.*, 2011). The results of this maximum-likelihood-based refinement (Read, 2001) are presented in Table 2. The final model of 357 non-H atoms, which also contains 25 water molecules, has a working *R* factor of 0.216 and an R_{free} of 0.284 at 1.85 Å resolution. H atoms were added to the molecule before refinement in riding positions. Bond-length, bond-angle and chiral volume deviations are all in good-to-acceptable ranges (see Table 2). The estimated coordinate error from maximum likelihood is 0.083 and that from the *R* factors is 0.220.

Table 3
Comparison of models: superposition of amino-acid residues 1–15 only.

Models	Mean deviation (Å)	R.m.s. deviation (Å)	Maximum deviation (Å)
Chain *A*/chain *B*	0.525	0.567	1.22
5glh/chain *A*	0.847	0.967	2.30
1edn/chain *A*	2.350	2.600	5.59
1edn/5glh	2.470	2.720	5.74

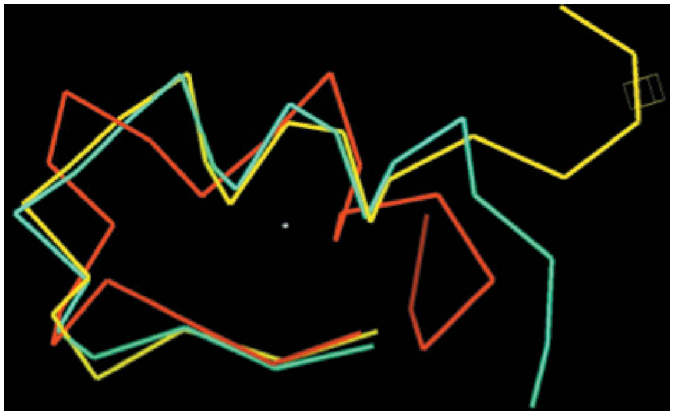

Figure 3
Model comparison. The backbone of the model presented here (yellow) is superimposed on the backbones of the models derived from PDB entry 5glh (Shihoya *et al.*, 2016; blue) and PDB entry 1edn (Janes *et al.*, 1994). Note particularly the divergence of the carboxy-terminal peptides.

The structural model of endothelin, and the asymmetric unit that emerged from the refinement, are shown in two representations in Fig. 2. The asymmetric unit consists of two molecules of the human hormone with attendant water molecules. Least-squares superposition (Emsley & Cowtan, 2004) of the main-chain atoms of one molecule (*A*) upon the other (*B*) in the asymmetric unit shows them to be virtually identical (r.m.s. difference of coordinates of 0.567 Å; mean deviation 0.525 Å; see Table 3). When the main-chain atoms (60 in number) of either of the two molecules are further superimposed upon the model of endothelin extracted from PDB entry 5glh, using only amino-acid residues 1–15 for fitting, the main-chain cores of the two structures, as seen in Fig. 3, are again almost the same (r.m.s. difference of 0.85 Å; mean deviation of 0.97 Å). There are significant differences, however, in the side-chain conformations. Superposition of all atoms of the model from PDB entry 5glh onto chain *A* or *B* yields an r.m.s. difference of 2.06 Å and a mean deviation of 1.54 Å. The uniform correspondence for main-chain atoms is hardly surprising given the profound constraints of the disulfide bonds. It is noteworthy that the carboxy-terminal 'tails' (amino-acid residues 16–21), although both in extended conformations (see Fig. 3), assume divergent directions in space.

Superficially, the models in Fig. 2 suggest that the pair of molecules in the asymmetric unit exhibit a twofold relationship. Closer inspection, however, reveals that this dyad is only very approximate. The two molecules are related by a pseudo-twofold axis that includes a slight shift of one molecule with respect to the other along the pseudo-dyad. Consider, for example, the relative positions of the prominent Tyr13 side chains of the two molecules in Fig. 2.

Although the 'core' backbones (amino-acid residues 1–15) of our endothelin model and that in PDB entry 5glh are virtually superimposable, the side chains are not. In Fig. 4(*a*), in which portions of the two models are superimposed, the large side chains of Lys9, Phe14 and His16 clearly have different rotameric conformations. In both molecules in the asymmetric unit, which were also refined independently with no NCS restraints applied, the φ, ψ angles for Ile19 in both the *A* and *B* chains were the only outliers in the Ramachandran plot (see Supplementary Fig. S2). Both consistently refined, however, to virtually the same model backbone angles even when altered to more canonical starting values. In both cases the electron density was convincingly supportive of the conformation in the model. No side-chain rotamers in the two molecules of 42 amino-acid residues appeared to be problematic, although several had little density to support them and probably had multiple conformations.

It is perhaps noteworthy that the carboxy-terminal tails of both molecules in the asymmetric unit, although flexible and extended, have very nearly the same conformation. The carboxy-terminal tryptophan side chain, which is shown with density superimposed upon it in Fig. 4(*d*) and which extends deep into the hydrophobic binding site of the receptor (Shihoya *et al.*, 2016), is particularly well ordered in chain *A* and its density is unambiguous. As the electrostatic surface representation in Fig. 5 shows, the dimer is highly hydrophobic, with only a few prominent charged groups visible. This hydrophobic character is also present in the monomer.

The dimer found in the asymmetric unit of these crystals may be stable in solution and may have physiological relevance, but we cannot be certain. The surface area buried as a consequence of dimerization is 532 Å^2 of a total surface area of 4064 Å^2, or about 12–13%. This is in the ambiguous region for stable oligomer formation (according to *PISA* in *CCP*4). It could also be a consequence of intermolecular interactions that form as a byproduct of crystal packing. Although the two molecules appear to be intimately paired, especially in the surface renderings (Fig. 5), the actual contacts between them are rather sparse. They mainly consist of contacts between Phe14 of one molecule and Leu17 of another, and between the side chain of Tyr13 of one molecule and the Cys1–Cys15 disulfide bond of the other. Dimer formation appears to be a result of the formation of a small intermolecular hydrophobic core between chains that in turn shields a number of side groups from water.

Principally because of the hydrophobic character of the molecule and the close packing, there are few associated waters. A rule of thumb is that about one to one and a half water molecules are observed per amino-acid residue in most crystalline proteins. The number here is therefore about 50% or less. The hydrophobicity is also reflected in the crystallization conditions, which included a temperature of 37°C. The 29% solvent content of the crystals is among the lowest of all entries in the PDB. Endothelin is not, in fact, a protein that is surrounded by several shells of solvent. It is a compact polypeptide hormone and its crystals share properties with crystals of conventional small molecules. The low solvent content and close packing of molecules are reflected in the relatively high clashscore. This score, in this instance, is dominated by what, in a protein structure, would be considered numerous 'close contacts' rather than prohibitive overlaps.

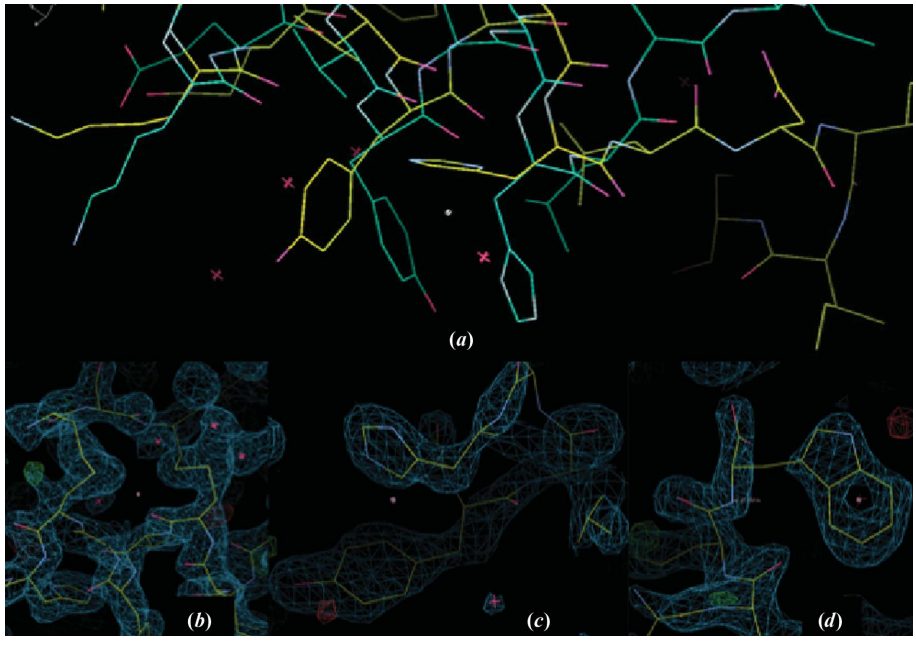

Figure 4
The electron density. In (*a*) a portion of the model presented here (yellow) is superimposed on the model from PDB entry 5glh (Shihoya *et al.*, 2016) and illustrates the many differences in side-chain conformations that are present, although the polypeptide backbones are virtually the same. (*b*), (*c*) and (*d*) show the fit of various segments of the molecule to the corresponding electron density. Of note is the well defined Trp21 side group at the carboxy-terminus of chain *A* in (*d*). Electron-density maps are contoured at 1.3 r.m.s.d. (0.56 e Å^{-3}).

There appears to be a short hydrogen bond of 2.12 Å between the ε-amino group of Lys9 of molecule *B* and the main-chain carbonyl oxygen of Met7 in a symmetry-related asymmetric unit. Finally, there is a close contact between the sulfur of Met7 in molecule *A* and the face of the side-chain ring of Tyr13 of molecule *B* in a symmetry-related asymmetric unit. Such a sulfur–aromatic ring interaction has for some time been recognized as a positive chemical interaction, or bond, in proteins (Reid *et al.*, 1985), and this appears to be the case here.

If the dimer of the crystals (a dimer was also seen in the analysis of PDB entry 1edn) is the dominant species *in vivo*, then it would have to dissociate prior to binding to the receptor. Alternatively, the receptor protein might promote its dissociation as part of the binding process. A second alternative is that the environment of the receptor is largely hydrophobic, in which case the dimer might spontaneously dissociate into monomers as a consequence of the destabilization of the hydrophobic core of the dimer.

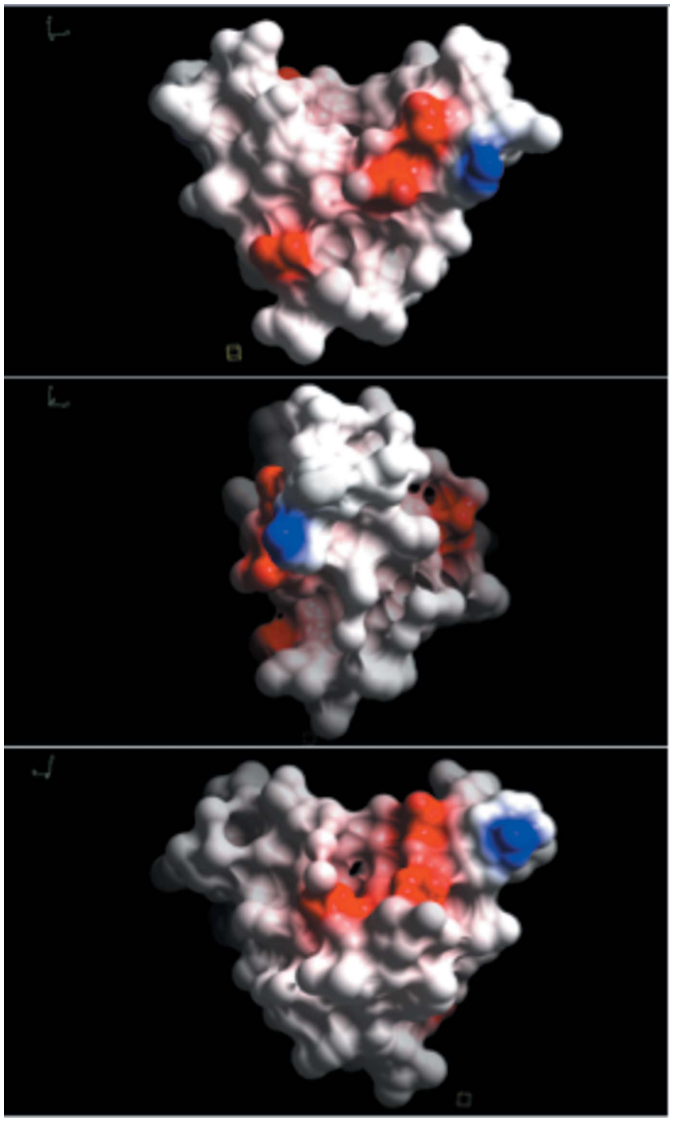

Figure 5
Electrostatic surfaces. Top: the endothelin dimer in the same orientation as in Fig. 1 presented as an electrostatic surface. Center: the molecule rotated by 90°. Bottom: the molecule rotated by a full 180°. It is evident that the molecule is extremely hydrophobic in character, with a paucity of exposed charged groups. C atoms are white, O atoms red and N atoms blue.

The structure of endothelin presented here (PDB entry 6dk5) is significantly different from the earlier crystal structure of the free molecule (PDB entry 1edn) in its core (amino-acid residues 1–15) and is very different in the carboxy-terminal tails. These differences may be ascribed to differences in crystallization conditions, crystal-packing interactions and general conformational flexibility. The carboxy-terminal 'tail', for example, is probably unstructured in solution and assumes its observed conformations only upon contact with the protein receptor or other endothelin molecules, as in the dimer found in these crystals.

It has been pointed out (Shihoya *et al.*, 2016) that the carboxy-terminal 'tail' makes contacts and positive interactions along its length with as many as 16 different amino-acid residues on the receptor when bound. This peptide, and especially the terminal tryptophan, although flexible, is clearly the 'trigger' that upon penetration into the receptor activates it to produce the vasoconstrictive effect. Presumably, this 'tail' peptide is restructured as a consequence of interactions with the protein receptor.

Acknowledgements

We wish to thank Duilio Cassio at UCLA for writing, specifically for us, the program that allowed us to convert old `.ARC` files from the SDMS processed data into `.MTZ` files suitable for scaling in *AIMLESS*.

References

Andersen, N. H., Chen, C., Marschner, T. M., Krystek, S. R. Jr & Bassolino, C. A. (1992). *Biochemistry*, **31**, 1280–1295.
Bagnato, A. & Rosanò, L. (2008). *Int. J. Biochem. Cell Biol.* **40**, 1443–1451.
Blessing, R. H. (1995). *Acta Cryst.* A**51**, 33–38.
Cody, W. L. & Doherty, A. M. (1995). *Biopolymers*, **37**, 89–104.
Davenport, A. P., Hyndman, K. A., Dhaun, N., Southan, C., Kohan, D. E., Pollock, J. S., Pollock, D. M., Webb, D. J. & Maguire, J. J. (2016). *Pharmacol. Rev.* **68**, 357–418.
Dhaun, N., Goddard, J., Kohan, D. E., Pollock, D. M., Schiffrin, E. L. & Webb, D. J. (2008). *Hypertension*, **52**, 452–459.
Ducancel, F. (2005). *Cell. Mol. Life Sci.* **62**, 2828–2839.
Emsley, P., Lohkamp, B., Scott, W. G. & Cowtan, K. (2010). *Acta Cryst.* D**66**, 486–501.
Evans, P. (2006). *Acta Cryst.* D**62**, 72–82.
Evans, P. R. (2011). *Acta Cryst.* D**67**, 282–292.
Evans, P. R. & Murshudov, G. N. (2013). *Acta Cryst.* D**69**, 1204–1214.
Gray, G. A. & Webb, D. J. (1996). *Pharmacol. Ther.* **72**, 109–148.
Hewage, C. M., Jiang, L., Parkinson, J. A., Ramage, R. & Sadler, I. H. (1997). *J. Pept. Sci.* **3**, 415–428.
Hickey, K. A., Rubanyi, G. R., Paul, R. J. & Highsmith, R. F. (1985). *Am. J. Physiol. Cell Physiol.* **248**, C550–C556.
Howard, A. J., Nielsen, C. & Xuong, N.-H. (1985). *Methods Enzymol.* **114**, 452–472.
Janes, R. W., Peapus, D. H. & Wallace, B. A. (1994). *Nature Struct. Biol.* **1**, 311–319.
Klabunde, T. & Hessler, G. (2002). *ChemBioChem*, **3**, 928–944.
Kloog, Y., Ambar, I., Sokolovsky, M., Kochva, E., Wollberg, Z. & Bdolah, A. (1988). *Science*, **242**, 268–270.

Kohan, D. E., Cleland, J. G., Rubin, L. J., Theodorescu, D. & Barton, M. (2012). *Life Sci.* **91**, 528–539.
Kuhn, H., Hubbard, A., Kannengieser, J. & Hackworth, C. (2006). *Georgetown Univ. J. Health Sci.* **3**.
Lüscher, T. F. & Barton, M. (2000). *Circulation*, **102**, 2434–2440.
Maguire, J. J. (2016). *Life Sci.* **159**, 30–33.
Maguire, J. J., Kuc, R. E. & Davenport, A. P. (2012). *Life Sci.* **91**, 681–686.
McCoy, A. J., Grosse-Kunstleve, R. W., Adams, P. D., Winn, M. D., Storoni, L. C. & Read, R. J. (2007). *J. Appl. Cryst.* **40**, 658–674.
McCoy, A. J., Grosse-Kunstleve, R. W., Storoni, L. C. & Read, R. J. (2005). *Acta Cryst.* D**61**, 458–464.
McPherson, A. (1982). *The Preparation and Analysis of Protein Crystals.* New York: John Wiley & Sons.
Murshudov, G. N., Skubák, P., Lebedev, A. A., Pannu, N. S., Steiner, R. A., Nicholls, R. A., Winn, M. D., Long, F. & Vagin, A. A. (2011). *Acta Cryst.* D**67**, 355–367.
Murshudov, G. N., Vagin, A. A. & Dodson, E. J. (1996). *Proceedings of the CCP4 Study Weekend. Macromolecular Refinement*, edited by E. Dodson, M. Moore, A. Ralph & S. Bailey, pp. 93–104. Warrington: Daresbury Laboratory.
Murshudov, G. N., Vagin, A. A. & Dodson, E. J. (1997). *Acta Cryst.* D**53**, 240–255.
Padilla, J. E. & Yeates, T. O. (2003). *Acta Cryst.* D**59**, 1124–1130.
Potenza, M. A., Addabbo, F. & Montagnani, M. (2009). *Am. J. Physiol. Endocrinol. Metab.* **297**, E568–E577.
Rautureau, Y. & Schiffrin, E. L. (2012). *Curr. Opin. Nephrol. Hypertens.* **21**, 128–136.
Read, R. J. (2001). *Acta Cryst.* D**57**, 1373–1382.
Reid, K. S. C., Lindley, P. F. & Thornton, J. M. (1985). *FEBS Lett.* **190**, 209–213.
Saudek, V., Hoflack, J. & Pelton, J. T. (1989). *FEBS Lett.* **257**, 145–148.
Shemyakin, A., Salehzadeh, F., Böhm, F., Al-Khalili, L., Gonon, A., Wagner, H., Efendic, S., Krook, A. & Pernow, J. (2010). *J. Clin. Endocrinol. Metab.* **95**, 2359–2366.
Shihoya, W., Nishizawa, T., Okuta, A., Tani, K., Dohmae, N., Fujiyoshi, Y., Nureki, O. & Doi, T. (2016). *Nature (London)*, **537**, 363–368.
Sokolovsky, M. (1995). *Cell. Mol. Neurobiol.* **15**, 561–571.
Storoni, L. C., McCoy, A. J. & Read, R. J. (2004). *Acta Cryst.* D**60**, 432–438.
Touyz, R. M. & Schiffrin, E. L. (2003). *Can. J. Physiol. Pharmacol.* **81**, 533–541.
Wallace, B. A., Janes, R. W., Bassolino, D. A. & Krystek, S. R. Jr (1995). *Protein Sci.* **4**, 75–83.
Waller, D., Cudney, R., Wolff, M., Day, J., Greenwood, A., Larson, S. & McPherson, A. (1992). *Acta Cryst.* B**48**, 239–240.
Winn, M. D., Ballard, C. C., Cowtan, K. D., Dodson, E. J., Emsley, P., Evans, P. R., Keegan, R. M., Krissinel, E. B., Leslie, A. G. W., McCoy, A., McNicholas, S. J., Murshudov, G. N., Pannu, N. S., Potterton, E. A., Powell, H. R., Read, R. J., Vagin, A. & Wilson, K. S. (2011). *Acta Cryst.* D**67**, 235–242.
Yanagisawa, M., Inoue, A., Ishikawa, T., Kasuya, Y., Kimura, S., Kumagaye, S., Nakajima, K., Watanabe, T. X., Sakakibara, S., Goto, K. & Masaki, T. (1988). *Proc. Natl Acad. Sci. USA*, **85**, 6964–6967.
Yanagisawa, M., Kurihara, H., Kimura, S., Tomobe, Y., Kobayashi, M., Mitsui, Y., Yazaki, Y., Goto, K. & Masaki, T. (1988). *Nature (London)*, **332**, 411–415.
Yanagisawa, M. & Masaki, T. (1989). *Trends Pharmacol. Sci.* **10**, 374–378.